



**HAL**  
open science

## Removal of the herbicide monolinuron from waters by the electro-Fenton treatment.

Pape Abdoulaye Diaw, Nihal Oturan, Mame Diabou Gaye Seye, Olivier Maurice Aly Mbaye, Moussa Mbaye, Atanasse Coly, Jean-Jacques Aaron, Mehmet Oturan

► **To cite this version:**

Pape Abdoulaye Diaw, Nihal Oturan, Mame Diabou Gaye Seye, Olivier Maurice Aly Mbaye, Moussa Mbaye, et al.. Removal of the herbicide monolinuron from waters by the electro-Fenton treatment.. Journal of Electroanalytical Chemistry, 2020, 864, pp.114087. 10.1016/j.jelechem.2020.114087 . hal-03261158

**HAL Id: hal-03261158**

**<https://hal.science/hal-03261158>**

Submitted on 22 Aug 2022

**HAL** is a multi-disciplinary open access archive for the deposit and dissemination of scientific research documents, whether they are published or not. The documents may come from teaching and research institutions in France or abroad, or from public or private research centers.

L'archive ouverte pluridisciplinaire **HAL**, est destinée au dépôt et à la diffusion de documents scientifiques de niveau recherche, publiés ou non, émanant des établissements d'enseignement et de recherche français ou étrangers, des laboratoires publics ou privés.



Distributed under a Creative Commons Attribution - NonCommercial 4.0 International License

## Removal of the herbicide monolinuron from waters by the electro-Fenton treatment

Pape Abdoulaye Diaw<sup>1,2,3</sup>, Nihal Oturan<sup>2</sup>, Mame Diabou Gaye Seye<sup>2,3</sup>, Olivier Maurice Aly Mbaye<sup>2,3</sup>, Moussa Mbaye<sup>3</sup>, Atanasse Coly<sup>3</sup>, Jean-Jacques Aaron<sup>2</sup>, Mehmet A. Oturan<sup>2,\*</sup>

<sup>1</sup> Laboratoire Matériaux, Electrochimie et Photochimie Analytique, Université A. Diop, Bambey, Sénégal.

<sup>2</sup> Université Paris-Est, Laboratoire Géomatériaux et Environnement (LGE), UPEM, 77454 Marne-la-Vallée, France.

<sup>3</sup> Laboratoire Photochimie et d'Analyse, Université C. A. Diop, Dakar, Sénégal.

\*Corresponding author Email: Mehmet.Oturan@univ-paris-est.fr

1

### 2 **Abstract:**

3 The removal of the phenylurea herbicide monolinuron (MLN) from water was investigated by  
4 the electro-Fenton method, based on the electro-catalytic *in situ* continuous production of  
5 large amounts of the strong oxidant hydroxyl radicals. The effect of several parameters,  
6 including the Fe<sup>2+</sup> initial concentration, applied current and type of anode (Pt and boron-  
7 doped diamond - BDD), on the MLN degradation kinetics was evaluated. MLN decay kinetics  
8 was monitored by HPLC, fitting a pseudo first-order reaction, leading to a rate constant  $k_{\text{abs}} =$   
9  $(3.1 \pm 0.2) 10^9 \text{ M}^{-1} \text{ s}^{-1}$ . Several oxidation intermediates species were identified and followed  
10 by HPLC and GC-MS. A quasi complete mineralization rate (98% TOC removal) of MLN  
11 solution was reached after 8 h of treatment on BDD anode with low energy consumption.  
12 Identification of carboxylic acids and inorganic ions was carried out by HPLC and ionic  
13 chromatography analyses. Based on identification of aromatic and aliphatic intermediates,  
14 inorganic end-products and TOC removal value, a complete MLN mineralization pathway  
15 was also proposed.

16 **Keywords:** Monolinuron; Electro-Fenton; Hydroxyl radicals; Degradation; Mineralization.

17

## 18 **1. INTRODUCTION**

19 Although pesticides and herbicides are utilized worldwide to protect crops, they also  
20 contribute significantly to the environmental pollution and their widespread use can cause  
21 serious health effects. Indeed, most pesticides do not reach their target and they can  
22 contaminate the atmosphere, surface waters and groundwater through various mechanisms  
23 such as volatilization, runoff, infiltration, etc. [1, 2].

24 Monolinuron (MLN) is a phenylurea herbicide, widely applied in agriculture, notably  
25 to control weeds in potato plantations [3]. Because of its relatively high hydro-solubility  
26 (Table 1), MLN possesses a great mobility in water, and, as a result, it constitutes a potential  
27 contaminant of water surface and ground waters. Numerous studies have revealed the  
28 presence of MLN in water as well as in food products [4-6]. For example, Traoré et al. [7]  
29 measured the mean contamination level of lagoon waters of Aghien and Potou in Ivory Coast  
30 and reported mean contamination level by eight substituted urea as  $121 \mu\text{g L}^{-1}$  where  
31 maximum concentration of MLN was around  $30 \mu\text{g L}^{-1}$ . MLN itself is not very toxic.  
32 Nevertheless, quality standards have been established to preserve human health. For example,  
33 the Directive 98/83/EC mentioned, for the quality standard for human health, a protective  
34 value of  $0.1 \mu\text{g L}^{-1}$  for drinking water and which is not based on the criteria of toxicology but  
35 rather of the limit of analytical quantification [8]. However, his degradation products,  
36 including aniline and *para*-chloroaniline (PCA), are considered as highly toxic and harmful to  
37 human health [9]. Therefore, it is of considerable interest to develop methods for  
38 decontamination of water polluted by such a persistent organics in order to ensure  
39 environmental safety. Advanced oxidation processes (AOPs) have been developed for

40 effective remediation of pesticides in soil and aqueous media [10-13]. Electro-Fenton (EF)  
41 process constitutes a potentially powerful AOP method which has been used in many studies  
42 for removing phenylurea pesticides, such as fenuron, monuron and diuron [14-16].

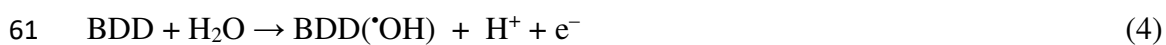
43 EF process is based on the Fenton's reaction (equation 1), which produces hydroxyl  
44 radicals ( $\cdot\text{OH}$ ) in the treated solution.  $\cdot\text{OH}$  are very powerful oxidizing agents, able to react  
45 with any organic compounds until their complete mineralization (i.e. their conversion into  
46  $\text{CO}_2$ ,  $\text{H}_2\text{O}$  and inorganic ions) [10]. In this process, firstly a catalytic amount of  $\text{Fe}^{2+}$  is  
47 introduced in the reaction medium, then hydrogen peroxide ( $\text{H}_2\text{O}_2$ ) is continuously generated  
48 *in situ* via electrochemical reduction of dissolved  $\text{O}_2$  (equation 2) [17-19]:



51 The Fenton's reaction can be maintained by means of a quick regeneration of the  $\text{Fe}^{2+}$   
52 (equation 3) based on the electrochemical reduction of  $\text{Fe}^{3+}$  formed in equation 1 [10]:



54 Carbon felt cathode and two anodes, including platinum (Pt) and boron doped diamond  
55 (BDD), have been successfully used in a number of studies for wastewater treatment by the  
56 EF process [19-21]. Due to its high  $\text{O}_2$  evolution over potential which allows to produce  
57 comparatively more amount heterogeneous hydroxyl radicals  $\text{M}(\cdot\text{OH})$  (equation 4), we will  
58 pay more attention to the BDD anode.  $\text{M}(\cdot\text{OH})$  is very efficient for mineralization of organics  
59 and specially short-chain carboxylic acids which are low affinity against homogeneous  $\cdot\text{OH}$   
60 [19, 21-23] generated in solution bulk.



62 To the best of our knowledge, the degradation of MLN by the EF process has never  
63 been reported. The main goal of this work was the treatment of MLN aqueous solution by the  
64 EF process using Pt and BDD anodes. MLN degradation kinetics was monitored by HPLC,  
65 and the mineralization ability of the process was assessed by measuring the total organic  
66 carbon (TOC) removed during electrolysis. Thereafter, oxidation intermediates were  
67 identified by GC-MS, and carboxylic acids and inorganic ions formed during mineralization  
68 were followed, respectively, by ion exclusion HPLC and by ionic chromatography analyses.  
69 This information allowed us to propose a plausible mineralization pathway of MLN by  
70 hydroxyl radicals in aqueous medium.

71

## 72 **2. MATERIAL AND METHODS**

### 73 **2.1 Chemicals**

74 MLN (3-(4-Chlorophenyl)-1-methoxy-1-methylurea, purity > 99%) (Table 1) and  
75 methanol were purchased from Sigma-Aldrich and were used as received. Carboxylic acids  
76 and other chemicals utilized in chromatographic analysis were supplied by Sigma-Aldrich,  
77 Fluka or Acros Organics (purity > 99%). Anhydrous sodium sulfate and anhydrous potassium  
78 sulfate (purity > 99%) were analytical grade and purchased from Sigma-Aldrich. They were  
79 used as catalyst and as supporting electrolyte. Sulfuric acid (purity > 98%) and hexahydrated  
80 Fe(II) sulfate as catalyst source (99.5%) were obtained from Acros Organics. All the MLN  
81 solutions were prepared with ultra-pure water, obtained from a Millipore Milli-Q system  
82 (resistivity > 18 M $\Omega$  cm at room temperature). 4-hydroxybenzoic acid (HBA) (purity =  
83 99.7%) from Prolabo was used as the competition substrate in the kinetic experiments.

84

### 85 **2.2 Electrochemical measurements**

86 A triple power supply (model HM7042-5, Germany) was used to monitor electrolyses  
87 and to measure the electrical charge consumed. Oxygen from compressed air was  
88 continuously supplied to the reaction medium by bubbling. Electrolyses were carried out in a  
89 230-mL cylindrical glass cell containing a MLN aqueous solution (0.1 mM). The cathode was  
90 a carbon felt piece covering the cell internal inner wall, and the anode was either a Pt  
91 cylindrical grid or a 24-cm<sup>2</sup> BDD sheet placed in the center of the electrochemical cell. A  
92 Na<sub>2</sub>SO<sub>4</sub> aqueous solution (50 mM) was used as electrolyte, and the pH of the medium was  
93 fixed at 3.0. Experiments were carried out in triplicate and the average values have been  
94 reported in the figures.

95

## 96 **2. 3. Instrumentation and analytical procedures**

### 97 *2.3.1 High performance liquid chromatography (HPLC)*

98 The MLN kinetic decay and evolution of some intermediates products were monitored  
99 by HPLC, using a Merck Lachrom liquid chromatograph, equipped with a diode array  
100 detector (DAD model L-7455), and fitted with a L-7100 model pump and a reverse-phase  
101 Purospher RP-18.5 μm, 4.6 mm (i.d.), 250 mm column placed in a L-7350 model oven  
102 (Merck) at 40°C. Chromatograms were treated with Ezchrome Elite software. The column  
103 was eluted with a water-methanol 35:65 v/v binary mixture mobile phase, at a flow rate of 0.7  
104 mL min<sup>-1</sup> and under a 170 bar pressure. The determination of MLN and intermediate products  
105 was performed by UV absorption at 240 nm. The generated aliphatic acids were identified and  
106 quantified by ion-exclusion HPLC, using an Altech liquid chromatograph equipped with a  
107 300-mm Supelcogel H column (ϕ = 7.8) and an UV absorption detector set at 225 nm. Mobile  
108 phase was a 1% H<sub>2</sub>SO<sub>4</sub> aqueous solution with flow rate of 0.2 mL min<sup>-1</sup>.

109

### 110 *2.3.2 Ionic chromatography*

111 Inorganic ions were analyzed by a Dionex ion chromatograph system (ICS-1000  
112 model), equipped with a conductivity detector thermostated at 35° C, an AS4A-SC ion  
113 exchange column (4 mm × 250mm) for anion analysis, and a CSRS 4 mm × 250 mm cation  
114 exchange column for cation analysis. Mobile phases were either a mixture of sodium  
115 bicarbonate (1.7 mM) and sodium carbonate (1.8 mM) for anion analysis, or a sulfuric acid (9  
116 mM) solution for cation analysis. Flow rate were fixed, respectively, at 2 and 1 mL min<sup>-1</sup>.

### 117 2.3.3 Total Organic Carbon (TOC)

118 Mineralization degree of the initial and electrolyzed samples was assessed from the  
119 decay of dissolved total organic carbon (TOC) measured with a Shimadzu, TOC-V analyzer.  
120 Total combustion of the samples was carried out at 680 °C in presence of a Pt catalyst.  
121 Oxygen was the carrier gas at 150 mL min<sup>-1</sup> flow rate. Mineralization percentages were  
122 determined according to the formula:

$$123 \text{Min (\%)} = \frac{\text{TOC}_0 - \text{TOC}_t}{\text{TOC}_0} \times 100 \quad (5)$$

124 where TOC<sub>0</sub> and TOC<sub>t</sub> were, respectively, the total organic carbon values at the initial time  
125 and at a time t.

126

### 127 2.3.4 Gas Chromatography-Mass Spectrometry (GC-MS)

128 MLN degradation by-products formed during the oxidative degradation were extracted with  
129 ethyl acetate and then identified by GC-MS analysis using a Thermo Fisher Scientific device,  
130 model ISQ-Trace-1300, equipped with an injector system split/splitless, and a 0.32-μm  
131 diameter and 15-m long column, kept in vacuum with a turbo-pump at high temperature (200  
132 -250 °C). The mobile phase (helium) flux was maintained constant in range of 0.6 to 1.5 μL  
133 min<sup>-1</sup>. A NIST library Xcalibur software was utilized to interpret the mass spectra (m/z values  
134 comprised between 50 and 650).

135

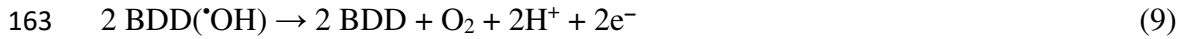
### 136 3. RESULTS AND DISCUSSION

#### 137 3.1 Kinetic study of the monolinuron degradation

138 Decay of MLN concentration was monitored by HPLC at a 240 nm absorption  
139 wavelength. Chromatogram showed a well-defined peak with a retention time of 6.9 min. The  
140 effects of applied current, catalyst concentration and type of anode on the MLN degradation  
141 kinetics were investigated.

142 The effect of current on the oxidative degradation of MLN and comparison of the  
143 influence of Pt and BDD anodes were performed using a 0.2 mM catalyst ( $\text{Fe}^{2+}$ ) concentration  
144 at pH 3. For both anodes, kinetic curves were characterized by a regular exponential decay of  
145 FLM concentration when the current increased from 50 mA to 500 mA (Fig. 1). As can be  
146 seen, the best degradation rate was reached at 250 and 300 mA for BDD and Pt anodes,  
147 respectively. MLN complete degradation took place after about 10 and 15 min electrolysis  
148 with BDD and Pt anodes, respectively. Degradation of MLN was significantly quicker than  
149 that obtained by Zouaghi et al. using sonocatalysis (over 40 min) [24] and heterogeneous  
150 photocatalysis using  $\text{TiO}_2$  under simulated solar irradiation ( $k_{\text{app}} = 0.035 \text{ min}^{-1}$ ) [25]. The  
151 better performance of BDD anode can be explained by its large  $\text{O}_2$ -evolution potential and  
152 physical adsorption inversely to Pt for which  $\text{M}(\cdot\text{OH})$  are chemisorbed and consequently less  
153 available. Degradation of MLN becomes slower for currents above these optimal values.  
154 Indeed, at high current values BDD( $\cdot\text{OH}$ ),  $\text{H}_2\text{O}_2$  and consequently  $\cdot\text{OH}$  were produced at high  
155 quantities due to enhancement of electrochemical reactions (Eqs. 1-4). High concentrations of  
156  $\text{H}_2\text{O}_2$  promote the wasting of  $\cdot\text{OH}$  in the bulk solution (Eqs. 6, 7) [12, 13]. On the other hand,  
157 high concentration of BDD( $\cdot\text{OH}$ ) leads to their wasting through Eqs. (8) and (9). Moreover, at  
158 high current values, the 4-electron reduction of  $\text{O}_2$  into  $\text{H}_2\text{O}$  (equation 10) can take place and  
159 compete with the formation of  $\text{H}_2\text{O}_2$  (equation 2) [26-28].





165 The effect of variation of catalyst ( $\text{Fe}^{2+}$ ) concentration from 0.05 to 0.5 mM on the  
 166 kinetic curves was investigated at the optimal current value with BDD anodes (Fig. 2). It can  
 167 be noted that the degradation kinetics was accelerated when the  $\text{Fe}^{2+}$  concentration increased  
 168 from 0.05 to 0.1 mM. A same kinetics behavior was obtained for 0.2 mM catalyst  
 169 concentration. But, Fig. 2 also showed that beyond 0.2 mM, the MLN degradation kinetics  
 170 was slowed due to the enhancement of parasitic reaction (equation 11) leading to the  
 171 consumption of formed  $\cdot\text{OH}$ . Moreover, the  $\text{Fe}^{3+}$  ions, formed from the Fenton reaction  
 172 (equation 1), can react with  $\text{H}_2\text{O}_2$ , leading to the formation of hydroperoxy radicals ( $\text{HO}_2\cdot$ )  
 173 (equation. 11) [11, 23], a less reactive oxidant than  $\cdot\text{OH}$ .



176 The influence of the type of anode on the MLN degradation kinetics was depicted in  
 177 Fig. 3. This figure shows also the comparison of degradation efficiency of the EF and anodic  
 178 oxidation (AO) treatments. Two results can be drawn from this figure: i) EF process is  
 179 significantly more efficient than AO process in degradation of MNL and b) EF process is  
 180 clearly more efficient with BDD anode than with Pt anode. This advantage of the BDD anode  
 181 over the Pt one can be related to its high amount of  $\text{M}(\cdot\text{OH})$  production (related to its large  
 182  $\text{O}_2$ -evolution overvoltage) compared to Pt anode and high reactivity of  $\text{BDD}(\cdot\text{OH})$  than  
 183  $\text{Pt}(\cdot\text{OH})$  which are strongly adsorbed to the anode surface and therefore less available to  
 184 oxidize MNL molecules. The efficiency of these treatments in the MLN degradation followed

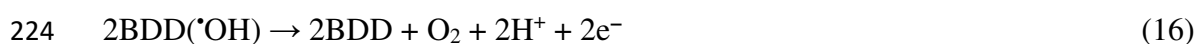
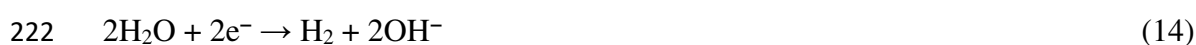
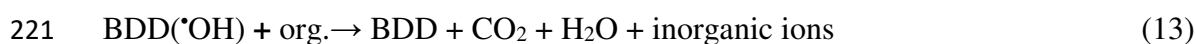
185 the order: AO-Pt < AO-BDD < EF-Pt < EF-BDD. A similar order of efficiency was already  
186 demonstrated by our group [15, 20] in the degradation of 2-chlorobenzoic acid and 2-  
187 nitrophenol in aqueous medium.

## 188 **3.2 Mineralization study of monolinuron**

### 189 *3.2.1 TOC removal kinetics*

190 To study the effect of current on the mineralization of MLN solution the electrolysis time was  
191 extended up to 8 h and the evolution of mineralization rate was followed by measuring the  
192 change of solution TOC with electrolysis time at different current values between 50 and  
193 1500 mA. As can be seen in Fig. 4, the mineralization rate strongly depended on the applied  
194 current, but also on the nature of the anode used in EF process. In the case of the BDD anode  
195 (Fig. 4a), the mineralization rate exceeded 98% for 500 mA whereas it was only 69.7% in the  
196 case of Pt anode (Fig. 4b) at 500 mA constant current electrolysis. The mineralization rate  
197 reached around 80% even for a current significantly higher such as 1500 mA. This important  
198 difference between the efficiency of both anodes was attributed to the high oxidizing power of  
199 BDD, which allowed a MLN complete oxidation, leading to a total mineralization of its  
200 aqueous solution according to equation 13. As reported by previous works [17, 29, 30], this  
201 result might be explained by the excellent mineralization power of BDD anode in relation to  
202 its, large O<sub>2</sub>-evolution overpotential (1.7 V) and availability of slightly adsorbed hydroxyl  
203 radicals, as already evoked in sub-section 3.1 [19]. These characteristics led to the rapid and  
204 easy formation of larger amount of heterogeneous BDD(<sup>•</sup>OH) radicals (equation 4) and a  
205 good reactivity with organic pollutants [17, 19, 31]. Inversely, in the case of Pt anode,  
206 mineralization could be limited by the chemisorption of <sup>•</sup>OH radicals on Pt surface, which  
207 reduced the oxidation capacity of Pt(<sup>•</sup>OH) radicals [17, 26]. Also, the applied current value  
208 probably played an important role in the anodic oxidation [26, 29]. One can see that, upon  
209 increasing the current from 100 to 500 mA, the TOC removal efficiency increased from 95 to

210 98% for the BDD anode. Obviously, the effect of current on mineralization rate is more  
 211 important in EF process with Pt anode: mineralization rate increased from 42.7% at 100 mA  
 212 to 69.7% at 500 mA. This indicates that the mineralization was promoted mainly by  
 213 homogeneous  $\cdot\text{OH}$  at low currents due to the formation of low amount of  $\text{Pt}(\cdot\text{OH})$ . In contrast,  
 214 the contribution of  $\text{Pt}(\cdot\text{OH})$  becomes more important at high current values as can be seen on  
 215 the Fig. 4b. In the case of BDD anode, the current efficiency was limited beyond 500 mA by  
 216 some parasitic reactions for which reaction rate is enhanced at high current values such  $\text{H}_2$   
 217 evolution (equation 14) and reduction of  $\text{H}_2\text{O}_2$  (equation 15) at the cathode and  $\text{O}_2$  evolution  
 218 (equation 16) as well as  $\text{H}_2\text{O}_2$  oxidation at the anode (equation 6) [10, 19]. These reactions  
 219 decrease mineralization efficiency of MNL solution in agreement with previous reports [18,  
 220 26].



### 225 3.2.2 Evolution of the carboxylic acids

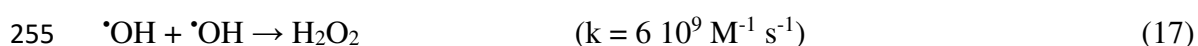
226 Several carboxylic acids, including oxalic, oxamic, formic, acetic, malonic and tartronic acids,  
 227 were detected during the mineralization of MLN and their identification and quantification  
 228 were performed by using standard solutions. Fig. 5 shows the different behavior of these acids  
 229 on the both types of anode.

230 In the case of the BDD anode, maximum concentrations of 0.005 mM for tartronic and  
 231 formic acids, 0.009 mM for malonic acid and 0.01 mM for acetic acid were reached after a  
 232 30-min electrolysis, whereas maximum concentrations of, respectively, 0.002 and 0.012 mM

233 for oxamic and oxalic acids were attained after a 60-min electrolysis. With the exception of  
234 formic acid, all these acids disappeared after 4 h of treatment (Fig. 5a).

235 For the Pt anode, concentrations of carboxylic acids were higher than those obtained  
236 with BDD anodes; the maximum concentrations were reached after 30-min electrolysis for,  
237 malonic and acetic acids at concentrations of 0.006 and 0.015 mM, respectively. For tartronic  
238 and oxalic acids, maximum concentrations of 0.012 and 0.026 mM, respectively, were  
239 attained after 60-min electrolysis. Formic and oxamic acid reached maximum concentrations  
240 of 0.016 and 0.005 mM, after 3 h and 4 h of electrolysis, respectively (Fig. 5b). Oxalic,  
241 oxamic and formic acids are known to be resistant to oxidation by  $\cdot\text{OH}$  [32] and constitute the  
242 residual TOC at the end of treatment.

243 It is well known that carboxylic acids have low affinity for homogeneous OH [10 ,17].  
244 Another reason is the formation of carboxylate-iron complexes which have a great resistance  
245 to oxidation by OH and present great stability in the case of Pt anode [23, 32, 33]. According  
246 to Sirés et al. [21], the carboxylato- $\text{Fe}^{2+}$  complexes can be destroyed by  $\cdot\text{OH}$  s whereas the  
247 carboxylato- $\text{Fe}^{3+}$  complexes can more efficiently destroyed by BDD( $\cdot\text{OH}$ ). Consequently,  
248 quick mineralization of carboxylic acids was noted in the case of BDD anode thanks to its  
249 high mineralization power [21, 33]. The high concentration of BDD( $\cdot\text{OH}$ ) on the anode  
250 surface and their relatively free character makes them more reactive against destruction of  
251 carboxylic acids. However, the degradation kinetic of carboxylic acids could be affected by  
252 wasting reactions such as recombination of homogeneous radicals (equation 17) and the  
253 destruction of the heterogeneous radicals BDD( $\cdot\text{OH}$ ) (equation 16) due to the presence of  
254 weak amounts of TOC in the medium at longer electrolysis times.



256 Nevertheless, all our results confirmed the very strong oxidative activity of the BDD  
257 anode and its greater effectiveness than the Pt anode for the treatment of MLN and its  
258 intermediates and end-products.

259

### 260 *3.2.3 Formation and Evolution of the inorganic ions*

261 Ionic chromatography was used for the detection and quantitative analysis of inorganic  
262 ions formed during the MLN mineralization. A comparative study of the behavior of these  
263 ions in the case of the BDD and Pt anodes was performed for MLN in the same experimental  
264 conditions than the monitoring of carboxylic acids.

265 As the MLN molecule contains Cl and N atoms, the formation of chloride ( $\text{Cl}^-$ ),  
266 ammonium ( $\text{NH}_4^+$ ) and nitrate ( $\text{NO}_3^-$ ) ions is expected during the mineralization experiments.  
267 The results are depicted in Fig. 6.

268 In the case of the BDD anode, the concentration of  $\text{Cl}^-$  ions increased and reached a  
269 maximum value of 0.08 mM (corresponding to 80% of the chlorine initial theoretical value)  
270 after 3 h of electrolysis, then decreased very rapidly, reaching 0.01 mM after 8 h. For  $\text{NO}_3^-$   
271 ions, a maximum concentration of about 0.05 mM was obtained after 1 h of electrolysis and  
272 then decreased progressively to a nil concentration after 8 h of electrolysis, whereas for  $\text{NH}_4^+$   
273 ions a maximum concentration of about 0.17 mM was reached after 4 h of electrolysis, and  
274 then increased slightly to reach 0.18 mM after 8 h of electrolysis (Fig. 6a).

275 For the Pt anode, the  $\text{Cl}^-$  ion concentration reached quickly to about 0.1 mM  
276 (corresponding to its initial theoretical value) after 2 h electrolysis and then remained constant  
277 inversely to that observed with BDD anode.  $\text{NO}_3^-$  and  $\text{NH}_4^+$  ions reached a maximum  
278 concentration of 0.043 and 0.15 mM, respectively, after about 3 h electrolysis and then  $\text{NH}_4^+$   
279 remained practically constant throughout the electrolysis whereas  $\text{NO}_3^-$  concentration  
280 decreased slightly (Fig. 6b). The decrease of  $\text{Cl}^-$  ions was observed by several authors [21, 30,

281 [32-34] when using BDD anode in electrochemical advanced oxidation processes (EF or AO)  
 282 due to the outstanding oxidation power of this anode. Indeed,  $\text{Cl}^-$  is quickly oxidized into  $\text{Cl}_2$   
 283 gas (equation 18), which was rapidly transformed into  $\text{HOCl}/\text{ClO}^-$  (equations 19 and 20) in  
 284 aqueous medium, an oxidant often used for water disinfection [35]. This phenomenon was not  
 285 observed with Pt anode since it is not able to oxidize effectively  $\text{Cl}^-$  ion. Then, as reported by  
 286 Randazzo et al. [36] during the comparative electrochemical treatments of two chlorinated  
 287 aliphatic hydrocarbons,  $\text{HOCl}/\text{ClO}^-$  can be consecutively transformed into less powerful  
 288 oxidant like  $\text{ClO}_3^-$  and  $\text{ClO}_4^-$  during oxidation processes

289 The decrease in  $\text{NO}_3^-$  concentration (more evident in the case of BDD anode) can be  
 290 related to its electrochemical reduction on the large surface carbon felt cathode into  $\text{NH}_4^+$   
 291 (equation 21). On the other side, the absence of nitrite ( $\text{NO}_2^-$ ) noted here may be due to the  
 292 presence of  $\text{Cl}^-$  ions. Indeed, Pérez et al [37] attributed the absence of  $\text{NO}_2^-$  ions to their  
 293 immediate oxidation into nitrate ( $\text{NO}_3^-$ ) ions by the action of hypochlorous acid ( $\text{HOCl}$ )  
 294 according to the equation 22, since the pH of the medium is about 3. In the same way, Wang  
 295 et al. [38] explained the absence of  $\text{NO}_2^-$  ions in the solution by their reaction with active  
 296 chlorine species formed from oxidation of chloride ions at the anode. The same author [38]  
 297 suggested also that the presence of  $\text{Cl}^-$  ions could prevent the accumulation of  $\text{NO}_2^-$  ions,  
 298 promoting their rapid and simultaneous oxidation into  $\text{NO}_3^-$  ions (equation 23). Several  
 299 authors demonstrated that the efficiency of  $\text{NO}_3^-$  removal depended to different parameters  
 300 such as the concentration of  $\text{Cl}^-$  ions, boron doping,  $\text{sp}^3/\text{sp}^2$  carbon ratio, etc. [39, 40].

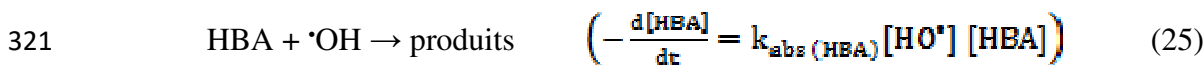
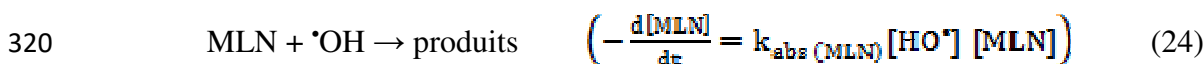




307

308 **3.3 Determination of the rate constant for MLN oxidation by  $\cdot\text{OH}$**

309 The absolute (second order) rate constant ( $k_{\text{abs(MLN)}}$ ) for oxidation of MLN by  $\cdot\text{OH}$   
 310 (equation 24) was determined by competition kinetics method using 4-hydroxybenzoic acid  
 311 (HBA) (equation 25) as the standard competitor with a well-known  $k_{\text{abs(HBA)}} = 2.19 \times 10^9\text{ M}^{-1}$   
 312  $\text{s}^{-1}$  [41]. These reactions were carried out with a BDD anode at 50 mA constant current and  
 313 same concentrations of MLN and HBA (0.1 mM) during the first ten minutes of electrolysis,  
 314 in order to avoid the interference of probable intermediate products. The evolution of FLM  
 315 and HBA was continuously followed by HPLC analysis. Assuming that only these two  
 316 bimolecular reactions took place between  $\cdot\text{OH}$  and MLN and between  $\cdot\text{OH}$  and HBA, and  
 317 that they obeyed to pseudo-first order kinetics, the combination of both rate constants ( $\text{Ln}$   
 318  $[\text{MLN}]_0/[\text{MLN}]_t = f(\text{Ln}([\text{HBA}]_0 / [\text{HBA}]_t))$  (equation 26) gave a linear plot (Fig. 7), of which  
 319 the slope led to the absolute rate constant value  $k_{\text{abs(MLN)}} = (3.1 \pm 0.2) 10^9\text{ M}^{-1}\text{ s}^{-1}$ .



322 
$$\text{Ln} \frac{[\text{MLN}]_0}{[\text{MLN}]_t} = \frac{k_{\text{abs(MLN)}}}{k_{\text{abs(HBA)}}} \times \text{Ln} \frac{[\text{HBA}]_0}{[\text{HBA}]_t}$$
 (26)

323 This large value of  $k_{\text{abs(MLN)}}$  is of the same order of magnitude than the absolute rate  
 324 constants of some other phenylurea pesticides, such as diuron, fenuron, linuron pesticides,  
 325 found by several authors using the electro-Fenton reaction or other advanced oxidation  
 326 processes [10,14, 42].

327 **3.4 Mineralization efficiency and Energy consumption**

328 Taking into account the quasi-complete mineralization (more than 98% TOC removal  
 329 with BDD anode) of MLN solution, we can write the following electrochemical  
 330 mineralization reaction:



332 Based TOC removal results and equation 27, we calculated the mineralization current  
 333 efficiency (MCE) [23, 43] and the energy consumption (EC) [15, 44] according to equations  
 334 28 and 29, respectively.

$$335 \text{MCE}(\%) = \frac{n F V_{\text{sol}} \Delta(\text{TOC})_{\text{exp}}}{4.32 * 10^7 m I t} * 100 \quad (28)$$

$$336 \text{EC} \left( \frac{\text{kWh}}{\text{gTOC}} \right) = \frac{U_{\text{cell}} * I * t}{V_{\text{sol}} * \Delta(\text{TOC})_{\text{exp}}} \quad (29)$$

337 where  $U_{\text{cell}}$  is the cell average voltage (V),  $I$  is the applied current (A),  $t$  is the electrolysis time  
 338 (h),  $V_{\text{sol}}$  is the solution volume (L),  $\Delta(\text{TOC})_{\text{exp}}$  is the experimental TOC decay ( $\text{mg L}^{-1}$ ),  $m$  is  
 339 the number of C atoms in the molecule MLN (9),  $F$  is the Faraday constant ( $96487 \text{ C mol}^{-1}$ ),  $n$   
 340 is the number of electrons exchanged and  $4.32 \cdot 10^7$  is the homogenization conversion factor  
 341 units ( $= 3600 \text{ s h}^{-1} \times 12000 \text{ mg C mol}^{-1}$ ).

342 Results obtained are depicted in Table 2, showing the great mineralization power of  
 343 electro-Fenton process with BDD anode. In fact, both higher MCE and lower EC values are  
 344 obtained with BDD anode. As can be seen from Table 2, the larger value of MCE and lower  
 345 value of EC in the case of electro-Fenton with BDD compared to that with Pt anode showed  
 346 the great importance of the type of anode in mineralization of organic pollutant.

347 These results also reflected the high oxidizing power of BDD due to the formation of  
 348 high amount additional BDD( $\cdot\text{OH}$ ) (equation 4), that could easily oxidize the carboxylic  
 349 acids, in contrast with the Pt( $\cdot\text{OH}$ ) having low mineralization power against these species [19,  
 350 20].



351 It is worthy to note that both anodes (BDD and Pt) give comparable and good  
352 degradation rate (with 10 and 15 min for complete degradation of 0.1 mM MLN,  
353 respectively). For only degradation purpose, Pt anode would be used instead of BDD anode  
354 which is more expensive. However, a significant difference has been noted during  
355 mineralization experiments where mineralization efficiency and EC were clearly better in the  
356 case of BDD anode that has also been already reported in the literature [45-48] for total  
357 removal of organics and their aromatic and aliphatic intermediates.

### 358 **3.5 Identification of by-products by HPLC and GC-MS**

359 Degradation of MLN by electro-Fenton led to the formation of several intermediate  
360 products detected by HPLC and/or GC-MS as shown in Table 3. Hydroquinone (1) and  
361 benzoquinone (2) were only detected by HPLC whereas p-hydroxyaniline (3), p-chloroaniline  
362 (4) and p-chlorophenol (5) were detected by both analysis methods. Besides some others  
363 intermediates such as p-chloroisocyanatobenzene (6), p-hydroxyphenylurea (7), p-  
364 chlorophenylurea (8), p-chlorophenylmethylurea (9), p-  
365 chlorophenylhydroxymethylmethoxyurea (10) and p-chlorophenylhydroxyméthylurea (11)  
366 were only monitored by GC-MS analysis.

367 It can be seen that MLN intermediates were formed from N-demethylation,  
368 hydroxylation and dechlorination reactions of the aromatic ring [49]. These degradation  
369 pathways have already been reported by some authors during mineralization of phenylurea  
370 pesticides [14, 49]. Further studies based on photolysis also described N-demethylation and  
371 hydroxylation as major routes of MLN degradation [50].

372 In fact, the N-demethoxylation and subsequent N-demethylation of MLN led,  
373 respectively, to (9) and (8). Similar degradation pathway leading to these two products was  
374 already suggested by Nelieu et al. [49] during the phototransformation of the MLN. Then, p-

375 hydroxyphenylurea (**7**) was formed by dechlorination of this latter intermediate by ipso attack  
376 of  $\cdot\text{OH}$  on -Cl position [51]. However, the breaking of the C-N bond of MLN led to  
377 elimination of N-methyl-methoxyaniline chain and formation of (**4**) and (**6**). These two by-  
378 products could also be obtained from (**8**) or (**9**), respectively, by breaking of the C-N bond of  
379 the carbonyl group followed by deamination. Chlorinated by-products as (**4**), (**6**), (**8**) and (**9**)  
380 are part of the MLN metabolites most commonly found in environmental matrices [24, 50].

381 On the other hand, the direct hydroxylation of the MLN aliphatic chain led to the  
382 formation of (**10**). The compound (**11**) is then formed from N-demethoxylation of (**10**). This  
383 latter product was also detected by Nélieu et al. [49] among the MLN photoproducts in  
384 aqueous media and could also be obtained by hydroxylation of (**9**). All oxidation pathways  
385 can conduct to the formation of (**4**), (**6**), (**5**) and (**3**) by elimination of aliphatic moieties under  
386 oxidative attacks of  $\cdot\text{OH}$  following H atom abstraction reaction mechanisms. Their further  
387 oxidations promote the formation of quinone derivatives, such as hydroquinone and  
388 benzoquinone, already highlighted by some authors [49, 52] whose oxidative ring opening  
389 reaction led to the formation of carboxylic acids. These latest were then completely oxidized  
390 into  $\text{CO}_2$ ,  $\text{H}_2\text{O}$  and inorganic ions at the end of treatment. The different pathways discussed  
391 above are depicted on Figure 8 which shows the oxidative degradation of MLN complete  
392 mineralization in aqueous solution during EF process.

393

#### 394 4. CONCLUSIONS

395 Electro-Fenton advanced oxidation process was used with success for the effective  
396 degradation and complete mineralization of MLN in aqueous medium. We have demonstrated  
397 that this treatment largely depended on the applied current and type of anode. Optimum  
398 degradation was obtained at 300 and 250 mA after 10 min of electrolysis, respectively, for Pt  
399 and BDD anodes. The initial catalyst concentration ( $\text{Fe}^{2+}$ ) constitutes an important parameter

400 because, beyond a concentration value of 0.1 mM, we noted a decrease of the degradation  
401 rate. The optimum mineralization rate (98%) was obtained with BDD anode at 500 mA, after  
402 8 h of electrolysis. In all cases, the MLN degradation reaction followed a pseudo-first order  
403 kinetic. The absolute rate constant for oxidation of MLN by  $\cdot\text{OH}$  was determined as  $3.1 \times 10^9$   
404  $\text{M}^{-1}\text{s}^{-1}$  indicating the great oxidizing power of hydroxyl radicals and the high capacity of the  
405 electro-Fenton process to complete mineralization of MNL solution. The monitoring by  
406 HPLC, ion chromatography and GC-MS analyses of the formation and evolution of aromatic  
407 and aliphatic (carboxylic acids) intermediates as well as end-products (TOC removal and  
408 inorganic ions) formed during the MLN electrolysis, allowed us to propose a plausible  
409 mineralization mechanism for MLN by  $\cdot\text{OH}$  generated in the process. Electro-Fenton with  
410 BDD electrode has demonstrated promising prospect during this study and will be applied in  
411 the future work to the treatment of surface and ground waters containing residual pesticides.

412

#### 413 **ACKNOWLEDGEMENTS**

414 One of the authors, Pape Abdoulaye Diaw, gratefully thanks the French Embassy in Senegal  
415 (Cooperation and Cultural Action Service) for a PhD grant.

416

## REFERENCES

- [1] J.M. Rousseau, M. Rüttimann, L. Brinquin, Intoxications aiguës par neurotoxiques organophosphorés: insecticides et armes chimiques. *Ann. Fr. Anesth. Réanim.* 19 (2000) 588–98.
- [2] E. Gauthier, I. Fortier, F. Courchesne, P. Pepin, J. Mortimer, D. Gauvreau, Environmental pesticide exposure as a risk factor for Alzheimer's disease: A case-control study. *Environ. Res.* 86 (2001) 37–45.
- [3] D. Freitag, I. Scheunert, Fate of [<sup>14</sup>C] monolinuron in potatoes and soil under outdoor conditions. *Ecotox. Environ. Safe.* 20 (1990) 256–268.
- [4] L. Guzzella, F. Pozzoni, G. Giuliano, Field Study on mobility and persistence of linuron and monolinuron in agricultural soil. *Inter. J. Environ. Anal. Chem.* 78:1 (2000) 87–106.
- [5] M.L. Escuderos-Morenas, M.J. Santos-Delgado, S. Rubio-Barroso, L.M. Polo-Díez, Direct determination of monolinuron, linuron and chlorbromuron residues in potato samples by gas chromatography with nitrogen-phosphorus detection. *J. Chromatogr. A* 1011 (2003) 143–153.
- [6] R. Devi, S.P. Sharma, A. Kumari, Pesticides contamination in potatoes and associated health risk to population with respect detection limits. *Inter. J. Food Sci. Nutr.* 3 (2018) 144–147.
- [7] A. Traoré, K.E. Ahoussi, N. Aka, Ad. TRAORE, N. Soro, Niveau de contamination par les pesticides des eaux des lagunes aghien et potou (sud-est de la côte d'ivoire). *Int. J. Pure App. Biosci.* 3 (4): (2015) 312-322.
- [8] INERIS. Maitriser le risque pour un développement durable. Monolinuron, validation groupe d'experts: Version 2, Octobre 2009.  
[http://europa.eu.int/comm/food/plant/protection/evaluation/existactive/list1-08\\_en.pdf](http://europa.eu.int/comm/food/plant/protection/evaluation/existactive/list1-08_en.pdf)
- [9] O. Osano, H.J.C. Klamerc, D. Pastorc, E.A.J. Bleeker, Comparative toxic and genotoxic effects of chloroacetanilides, formamidines and their degradation products on *Vibrio fischeri* and *Chironomus riparius*. *Environ. Pollut.* 119 (2002) 195–202.
- [10] M.A. Oturan, J.-J. Aaron, Advanced oxidation processes in water/wastewater treatment: Principles and applications. A Review, *Crit. Rev. Environ. Sci. Technol.* 44 (2014) 2577-2641.

- [11] M.A. Rodrigo, N. Oturan, M.A. Oturan, Electrochemically assisted remediation of pesticides in soils and water: A review. *Chem. Rev.* 114 (2014) 8720–8745.
- [12] S. Malato, P.F. Ibanez, M.I. Maldonado, J. Blanco, W. Gernjak, Decontamination and disinfection of water by solar photocatalysis: Recent overview and trends. *Catal. Today.* 147 (2009) 1–59.
- [13] E. Mousset, N. Oturan, E.D. Van Hullebusch, G. Guibaud, G. Esposito, M.A. Oturan, Influence of solubilizing agents (cyclodextrin or surfactant) on phenanthrene degradation by electro-Fenton process - study of soil washing recycling possibilities and environmental impact. *Water Res.* 48 (2014) 306–316.
- [14] M.A. Oturan, M.C. Edelahi, N. Oturan, K. El Kacemi, J.-J. Aaron, Kinetics of oxidative degradation/mineralization pathways of the phenylurea herbicides diuron, monuron and fenuron in water during application of the electro-Fenton process. *Appl. Catal. B: Environ.* 97 (2010) 82–89.
- [15] M.A. Oturan, N. Oturan, M.C. Edelahi, F.I. Podvorica, K. El Kacemi, Oxidative degradation of herbicide diuron in aqueous medium by Fenton's reaction based advanced oxidation processes. *Chem. Eng. J.* 171 (2011) 127–135.
- [16] E. Bringas, J. Saiz, I. Ortiz, Kinetics of ultrasound-enhanced electrochemical oxidation of diuron on boron-doped diamond electrodes. *Chem. Eng. J.*, 172 (2011) 1016–1022.
- [17] E. Brillas, I. Sirés, M.A. Oturan, Electro-Fenton process and related electrochemical technologies based on Fenton's reaction chemistry. *Chem. Rev.* 109 (2009) 6570–6631.
- [18] I. Sirés, E. Brillas, M.A. Oturan, M.A. Rodrigo, M. Panizza, Electrochemical advanced oxidation processes: today and tomorrow. A review. *Environ. Sci. Pollut. Res.* 21 (2014) 8336–8367.
- [19] N. Oturan, E. Brillas, M.A. Oturan, Unprecedented total mineralization of atrazine and cyanuric acid by anodic oxidation and electro-Fenton with a boron-doped diamond anode. *Environ. Chem. Lett.* 10 (2012) 165–170.
- [20] N. Oturan, M. Hamza, S. Ammar, R. Abdelhédi, M.A. Oturan, Oxidation/mineralization of 2-nitrophenol in aqueous medium by electrochemical advanced oxidation processes using Pt/carbon-felt and BDD/carbon-felt cells. *J. Electroanal. Chem.* 661 (2011) 66–71.

- [21] I. Sirés, N. Oturan, M.A. Oturan, R.M. Rodriguez, J.A. Garrido, E. Brillas, Electro-Fenton degradation of antimicrobials triclosan and triclocarban. *Electrochim. Acta* 52 (2007) 5493–5503.
- [22] A. Urtiaga, P.F. Castro, P. Gómez, I. Ortiz, Remediation of wastewaters containing tetrahydrofuran. Study of the electrochemical mineralization on BDD electrodes. *Chem. Eng. J.* 239 (2014) 341–350.
- [23] E. Brillas, B. Boye, I. Sirès, J.A. Garrido, R.M. Rodriguez, C. Arias, P.L. Cabot, C. Comninellis, Electrochemical destruction of chlorophenoxy herbicides by anodic oxidation and electro-Fenton using a boron-doped diamond electrode. *Electrochim. Acta* 49 (2004) 4487–4496.
- [24] R. Zouaghi, A. Zertal, B. David and S. Guittonneau, Photocatalytic degradation of monolinuron and linuron in an aqueous suspension of titanium dioxide under simulated solar irradiation. *Revue des Sciences de l'Eau / Journal of Water Science*, 20:2 (2007) 163-172.
- [25] R. Zouaghi, B. David, J. Suptil, K. Djebbar, A. Boutit, S. Guittonneau, Sonochemical and sonocatalytic degradation of monolinuron in water. *Ultrason. Sonochem.* 18 (2011) 1107-1112.
- [26] A. Özcan, M. A. Oturan, N. Oturan, Y. Şahin, Removal of Acid Orange 7 from water by electrochemically generated Fenton's reagent. *J. Hazard. Mater.* 163 (2009) 1213–1220.
- [27] A. Özcan, Y. Sahin, A. S. Koparal, M. A. Oturan, Carbon sponge as a new cathode material for the electro-Fenton process: Comparison with carbon felt cathode and application to degradation of synthetic dye basic blue 3 in aqueous medium. *J. Electroanal. Chem.* 616 (2008) 71–78.
- [28] E. Brillas, J.C. Calpe, J. Casado, Mineralization of 2,4-D by advanced electrochemical oxidation processes. *Water Res.* 34 (2000) 2253–2262.
- [29] X. Yu, M. Zhou, Y. Hu, K.G. Serrano, F. Yu, Recent updates on electrochemical degradation of bio-refractory organic pollutants using BDD anode: a mini review. *Environ. Sci. Pollut. Res.* 21 (2014) 8417–8431.
- [30] F. Sopaj, N. Oturan, J. Pinson, F. Podvorica, M.A. Oturan, Effect of the anode materials on the efficiency of the electro-Fenton process for the mineralization of the antibiotic sulfamethazine. *Appl. Catal. B: Environ.* 199 (2016) 331–341.

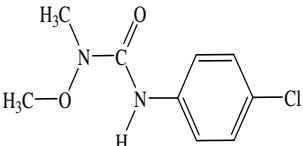
- [31] A. Dirany, I. Sirés, N. Oturan, A. Özcan, M.A. Oturan, Electrochemical treatment of the antibiotic sulfachloropyridazine: Kinetics, reaction pathways, and toxicity Evolution. *Environ. Sci. Technol.* 46 (2012) 4074–4082.
- [32] B. Boye M.M., Dieng, E. Brillas, Anodic oxidation, electro-Fenton and photoelectro-Fenton treatments of 2,4,5-trichlorophenoxyacetic acid. *J. Electroanal. Chem.* 557 (2003) 135–146.
- [33] M.A. Oturan, M. Pimentel, N. Oturan, I. Sirés, Reaction sequence for the mineralization of the short-chain carboxylic acids usually formed upon cleavage of aromatics during electrochemical Fenton treatment. *Electrochim. Acta* 54 (2008b) 173–182.
- [34] A. Kraft, M. Stadelmann, M. Blaschke, Anodic oxidation with doped diamond electrodes: a new advanced oxidation process. *J. Hazard. Mater.* 103 (2003) 247–261.
- [35] S. Koseki, K. Yoshida, S. Isobe, I. Kazuhiko, Decontamination of Lettuce Using Acidic Electrolyzed Water. *J. Food Prot.* 64 (5) (2001) 652–658.
- [36] S. Randazzo, O. Scialdone, E. Brillas, I. Sirés, Comparative electrochemical treatments of two chlorinated aliphatic hydrocarbons. Time course of the main reaction by-products. *J. Hazard. Mater.* 192 (2011) 1555–1564.
- [37] G. Pérez, R. Ibáñez, A.M. Urriaga, I. Ortiz, Kinetic study of the simultaneous electrochemical removal of aqueous nitrogen compounds using BDD electrodes. *Chem. Eng. J.* 197 (2012) 475–482.
- [38] D.M. Wang, H.Y. Lina, S.I. Shah, C.Y. Ni, C.P. Huang, Indirect electrochemical reduction of perchlorate and nitrate in dilute aqueous solutions at the Ti–water interface. *Sep. Purif. Technol.* 67 (2009) 127–134.
- [39] E. Lacasa, J. Llanos, P. Cañizares, M.A. Rodrigo, Electrochemical denitrification with chlorides using DSA and BDD anodes. *Chem. Eng. J.* 184 (2012) 66–71.
- [40] S. Garcia-Segura, M. Lanzarini-Lopes, K. Hristovski, P. Westerhoff, Electrocatalytic reduction of nitrate: Fundamentals to full scale water treatment applications. *Appl. Catal. B: Environ.* 236 (2018) 546–568.
- [41] M. Haidar, A. Dirany, I. Sirés, N. Oturan, M.A. Oturan, Electrochemical degradation of the antibiotic sulfachloropyridazine by hydroxyl radicals generated at a BDD anode. *Chemosphere* 91 (2013) 1304–1309.
- [42] K. Djebbar, T. Sehli, P. Mazellier, J.D. Laat, Phototransformation of diuron in aqueous solution by UV irradiation in the absence and in the presence of H<sub>2</sub>O<sub>2</sub>. *Environ. Technol.* 24 (2003) 479–489.

- [43] M. Panizza, A. Barbucci, M. Delucchi, M.P. Carpanese, A. Giuliano, M.C. Hernandez, G. Cerisola, Electro-Fenton degradation of anionic surfactants. *Sep. Purif. Technol.* 118 (2013) 394–398.
- [44] M. Panizza, E. Brillas, C. Comninellis, Application of boron-doped diamond electrodes for wastewater treatment. *J. Environ. Eng. Manage.* 18 (3) (2008) 139-153.
- [45] L. Ciríaco, C. Anjo, J. Correia, M.J. Pacheco, A. Lopes, Electrochemical degradation of Ibuprofen on Ti/Pt/PbO<sub>2</sub> and Si/BDD electrodes. *Electrochim. Acta* 54 (2009) 1464–1472.
- [46] Z. Frontistis, C. Brebou, D. Venieri, D. Mantzavinos, A. Katsaounis, BDD anodic oxidation as tertiary wastewater treatment for the removal of emerging micro-pollutants, pathogens and organic matter. *J Chem. Technol. Biotechnol.* 86 (2011) 1233–1236.
- [47] M.F. Wu, G.H. Zhao, M.F. Li, L. Liu, D.M. Li, Applicability of boron doped diamond electrode to the degradation of chloride-mediated and chloride-free wastewaters. *J. Hazard. Mater.* 163 (2009) 26–31.
- [48] C.A. Martínez-Huitle, E. Brillas, Decontamination of wastewaters containing synthetic organic dyes by electrochemical methods: a general review. *Appl. Catal. B Environ.* 87 (2009) 105–145.
- [49] S. Néliu, L. Kerhoas, M. Sarakha, J. Einhorn, Nitrite and nitrate induced photodegradation of monolinuron in aqueous solution. *Environ. Chem. Let.* 2 (2004) 83–87.
- [50] M.A. Oturan, M.C. Edelahe, N. Oturan, K. El kacemi, J.-J. Aaron, Kinetics of oxidative degradation/mineralization pathways of the phenylurea herbicides diuron, monuron and fenuron in water during application of the electro-Fenton process. *Appl. Catal. B: Environ.* 97 (2010) 82–89.
- [51] E. Mousset, N. Oturan, M.A. Oturan, An unprecedented route of •OH radical reactivity: ipso-substitution with perhalogenocarbon compounds. *Appl. Catal. B: Environ.* 226 (2018) 135–156.
- [52] M. Pimentel, N. Oturan, M. Dezotti, M.A. Oturan, Phenol degradation by advanced electrochemical oxidation process electro-Fenton using a carbon felt cathode. *App. Catal. B: Environ.* 83 (2008) 140–149.



## Table captions

**Table 1.** Some physicochemical properties of monolinuron.

Chemical formula	Molecular structure	Molecular weight (g mol <sup>-1</sup> )	Solubility (mg L <sup>-1</sup> ) in water at 25°C	Log K <sub>ow</sub> at 25°C
C <sub>9</sub> H <sub>11</sub> ClN <sub>2</sub> O <sub>2</sub>		214.65	735	2.3

**Table 2.** Energy consumption (EC) and mineralization current efficiency (MCE) during the electro-Fenton and anodic oxidation treatments of 0.1 mM MLN solution after 8 h of electrolysis. V = 230 ml; pH = 3; I = 500 mA.

Type of Process	TOC reduction (%)	EC (kWh (g TOC) <sup>-1</sup> )	MCE (%)
AO-BDD	97.0	10.2 ± 0.3	23.9
EF-Pt	69.7	12.4 ± 0.4	17.2
EF-BDD	98.2	10.0 ± 0.3	24.2

**Table 3.** HPLC and GC-MS detection of monolinuron (0.1 mM) and its metabolites formed during electro-Fenton treatment. Fe<sup>2+</sup> 0.1 mM, Na<sub>2</sub>SO<sub>4</sub> 50 mM; pH 3, V = 230 mL.

Compounds	HPLC	GC-MS	(m/z)	Structures
	R <sub>t</sub> (min)	R <sub>t</sub> (min)		
Monolinuron	7.04	18.18	214	
Hydroquinone (1)	3.53	-----	-----	
Benzoquinone (2)	3.77	-----	-----	
p-hydroxyaniline (3)	3.33	19.27	109	
p-chloroaniline (4)	5.56	19.47	127	
p-chlorophenol (5)	6.37	18.06	128	
p-chloroisocyanatobenzene (6)	-----	10.12	153	
p-hydroxyphenylurea (7)	-----	13.88	152	
p-chlorophenylurea (8)	-----	19.18	170	
p-chlorophenylmethylurea (9)	-----	19.47	184	
p-chlorophenylhydroxymethyl methoxyurea (10)	-----	20.16	231	
p-chlorophenylhydroxymethylurea (11)	-----	21.0	201	

R<sub>t</sub> = retention time

## Figure captions

**Fig. 1-** Effect of current on MLN during electro-Fenton treatment of 0.1 mM MLN solution with BDD (a) and Pt (b) anodes at 500 mA.  $[\text{Na}_2\text{SO}_4] = 50 \text{ mM}$ ;  $[\text{Fe}^{2+}] = 0.2 \text{ mM}$ ;  $\text{pH} = 3$ ;  $V = 230 \text{ mL}$ .

**Fig. 2-** Effect of catalyst ( $\text{Fe}^{2+}$ ) concentration on degradation kinetics of MLN with BDD anode.  $[\text{Fe}^{2+}]$  (mM): 0.05 (◆), 0.1 (■), 0.2 (▲), 0.5 (●). Experimental conditions:  $[\text{MLN}]_0 = 0.1 \text{ mM}$ ,  $I = 250 \text{ mA}$ ,  $[\text{Na}_2\text{SO}_4] = 50 \text{ mM}$ ,  $\text{pH} = 3$ ,  $V = 230 \text{ mL}$ .

**Fig. 3-** Evolution of MLN degradation kinetics during anodic oxidation (AO) and electro-Fenton (EF) treatments under constant current of 200 mA: AO/Pt (Δ), AO/BDD (▲), EF/Pt (□); EF/BDD (■).  $[\text{MLN}]_0 = 0.1 \text{ mM}$ ;  $[\text{Fe}^{2+}] = 0.1 \text{ mM}$  (only in the case of EF process);  $[\text{Na}_2\text{SO}_4] = 50 \text{ mM}$ ;  $\text{pH} = 3$ ;  $V = 230 \text{ mL}$ .

**Fig. 4-** Effect of the applied current on the MLN mineralization rate in terms of TOC removal at different electrolysis times during the electro-Fenton process with BDD (a) and Pt (b) anodes.  $[\text{MLN}]_0 = 0.1 \text{ mM}$ ,  $[\text{Fe}^{2+}] = 0.1 \text{ mM}$ ,  $\text{Na}_2\text{SO}_4 50 \text{ mM}$ ;  $\text{pH} = 3$ ,  $V = 230 \text{ mL}$ .

**Fig. 5-** Evolution of carboxylic acids formed during the mineralization of 0.1 mM of MLN by electro-Fenton process with (a) BDD anode, (b) Pt anode.  $I = 500 \text{ mA}$ ;  $[\text{Fe}^{2+}] = 0.1 \text{ mM}$ ;  $[\text{Na}_2\text{SO}_4] = 50 \text{ mM}$ ;  $\text{pH} = 3$ ;  $V = 230 \text{ mL}$ .

**Fig. 6-** Evolution of the inorganic ions:  $\text{Cl}^-$  (●),  $\text{NH}_4^+$  (▲) and  $\text{NO}_3^-$  (■) formed during the electro-Fenton treatment of 0.1 mM MLN solution with BDD (a) and Pt (b) anodes.  $I = 500 \text{ mA}$ .  $[\text{Fe}^{2+}] = 0.1 \text{ mM}$ ;  $[\text{K}_2\text{SO}_4] = 25 \text{ mM}$ ;  $\text{pH} = 3$ ;  $V = 230 \text{ mL}$ .

**Fig. 7-** Determination of the absolute rate constant of the MLN oxidation reaction by the hydroxyl radicals generated by the electro-Fenton process with Pt anode.  $I = 50 \text{ mA}$ ;  $[\text{Fe}^{2+}] = 0.2 \text{ mM}$ ;  $[\text{Na}_2\text{SO}_4] = 50 \text{ mM}$ ;  $\text{pH} = 3$ ;  $V = 230 \text{ mL}$ .

**Fig. 8-** Proposed mechanism for the mineralization of MLN in aqueous solution by electro-Fenton process.  $[\text{MLN}]_0 = 0.1 \text{ mM}$ ,  $[\text{Fe}^{2+}] = 0.1 \text{ mM}$ ,  $\text{Na}_2\text{SO}_4 50 \text{ mM}$ ;  $\text{pH} = 3$ ,  $V = 230 \text{ mL}$ , BDD anode,  $I = 500 \text{ mA}$ .

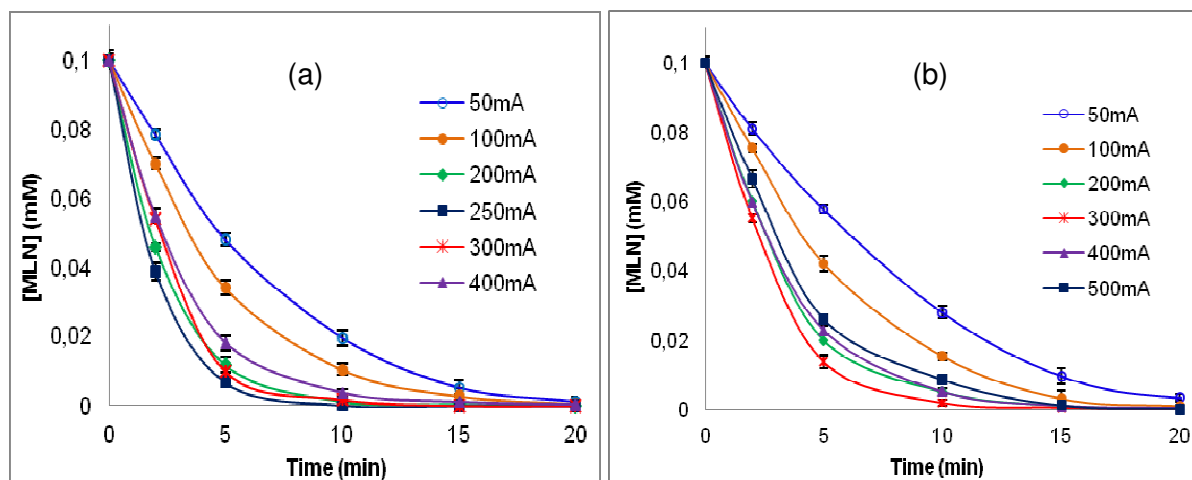


**Fig. 1-** Effect of current on MLN degradation kinetics during EF treatment of 0.1 mM MLN with BDD (a) and Pt (b) anodes at 500 mA.  $[\text{Na}_2\text{SO}_4] = 50 \text{ mM}$ ;  $[\text{Fe}^{2+}] = 0.2 \text{ mM}$ ;  $\text{pH} = 3$ ;  $V = 230 \text{ mL}$

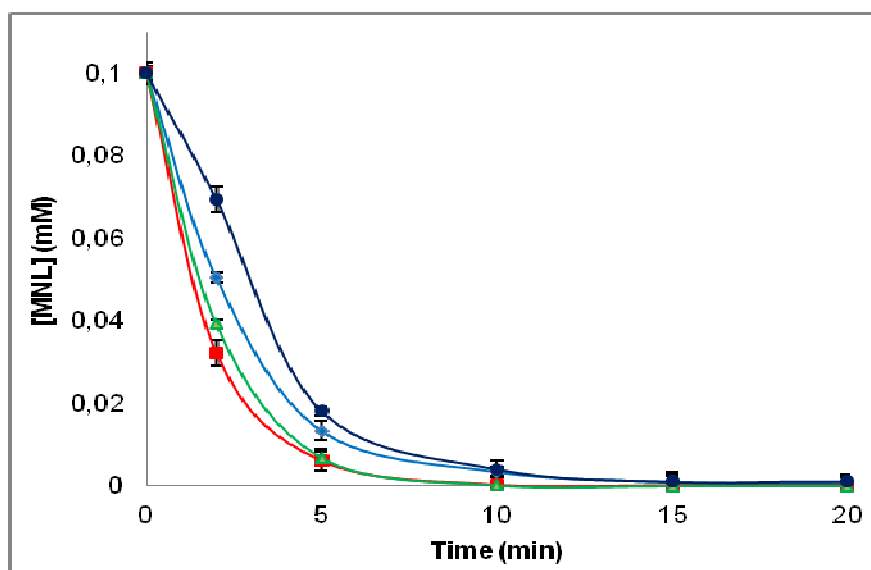


**Fig. 2-** Effect of catalyst ( $\text{Fe}^{2+}$ ) concentration on degradation kinetics of MLN with BDD.  $[\text{Fe}^{2+}]$  (mM): 0.05 ( $\blacklozenge$ ), 0.1 ( $\blacksquare$ ), 0.2 ( $\blacktriangle$ ), 0.5 ( $\bullet$ ). Experimental conditions:  $[\text{MLN}]_0 = 0.1 \text{ mM}$ ,  $I = 250 \text{ mA}$ ,  $[\text{Na}_2\text{SO}_4] = 50 \text{ mM}$ ,  $\text{pH} = 3$ ,  $V = 230 \text{ mL}$ .

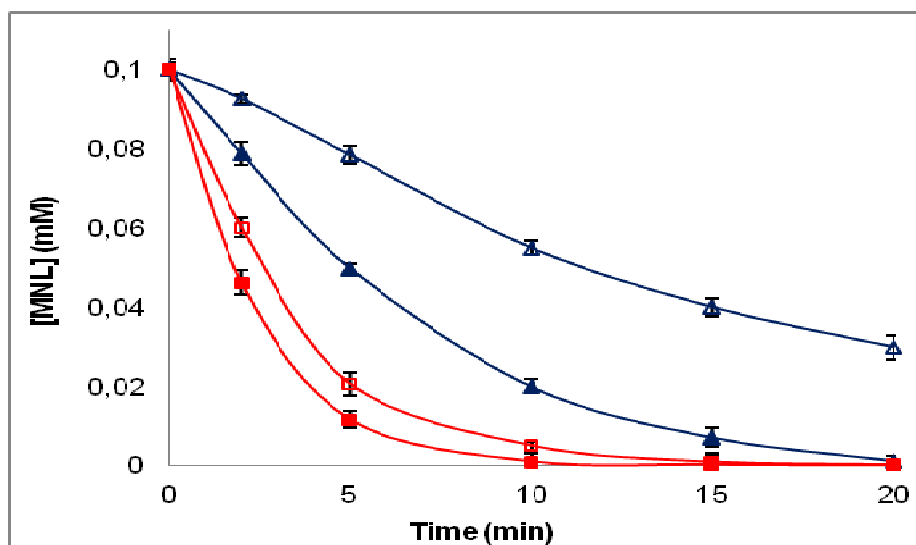


**Fig. 3-** MLN degradation kinetics during the anodic oxidation (AO) and electro-Fenton (EF) treatments under constant current of 200 mA: AO/Pt ( $\Delta$ ), AO/BDD ( $\blacktriangle$ ), EF/Pt ( $\square$ ); EF/BDD ( $\blacksquare$ ).  $[\text{MLN}]_0 = 0.1 \text{ mM}$ ;  $[\text{Fe}^{2+}] = 0.1 \text{ mM}$  (only in the case of EF process);  $[\text{Na}_2\text{SO}_4] = 50 \text{ mM}$ ;  $\text{pH} = 3$ ;  $V = 230 \text{ mL}$ .

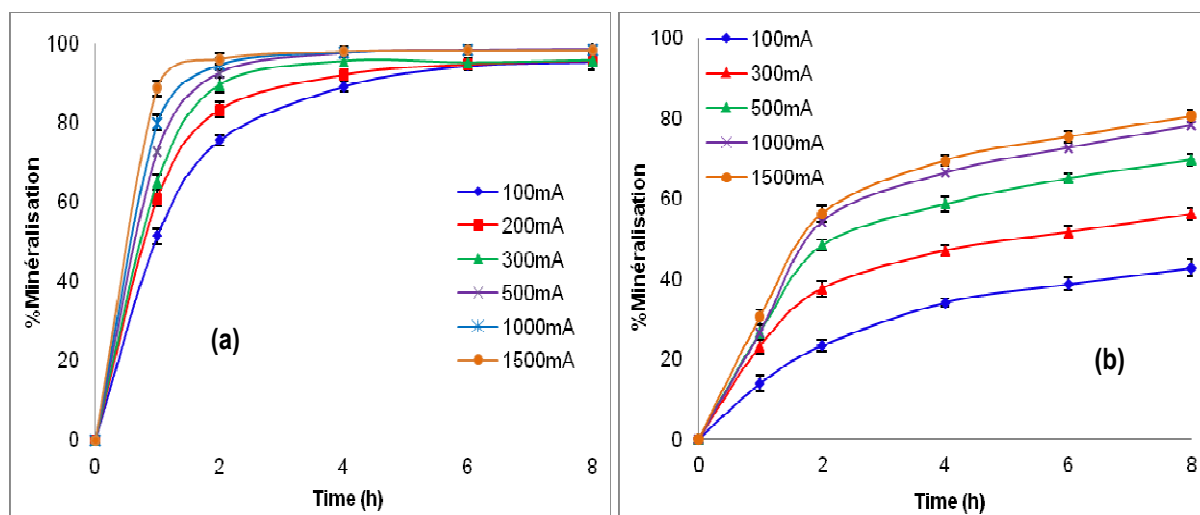


**Fig. 4-** Effect of the applied current on the MLN mineralization rate in terms of TOC removal at different electrolysis times during the electro-Fenton process with BDD (a) and on Pt (b) anodes.  $[\text{MLN}]_0 = 0.1 \text{ mM}$ ,  $[\text{Fe}^{2+}] = 0.1 \text{ mM}$ ,  $\text{Na}_2\text{SO}_4$  50 mM;  $\text{pH} = 3$ ,  $V = 230 \text{ mL}$ .

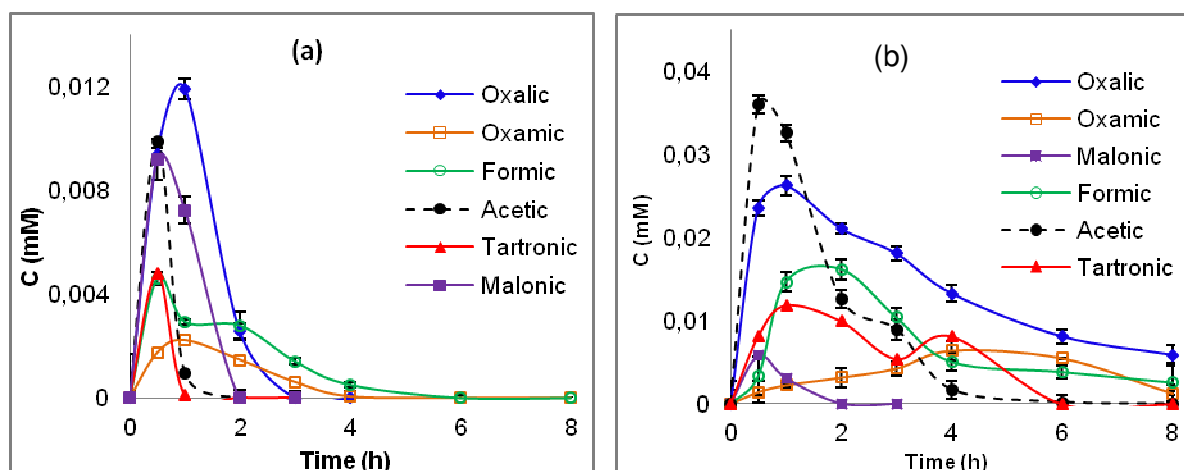


**Fig. 5-** Evolution of carboxylic acids formed during the mineralization of 0.1 mM MLN by the electro-Fenton process with BDD (a) and Pt (b) anodes at 500 mA constant current.  $[\text{Fe}^{2+}] = 0.1 \text{ mM}$ ;  $[\text{Na}_2\text{SO}_4] = 50 \text{ mM}$ ;  $\text{pH} = 3$ ;  $V = 230 \text{ mL}$ .

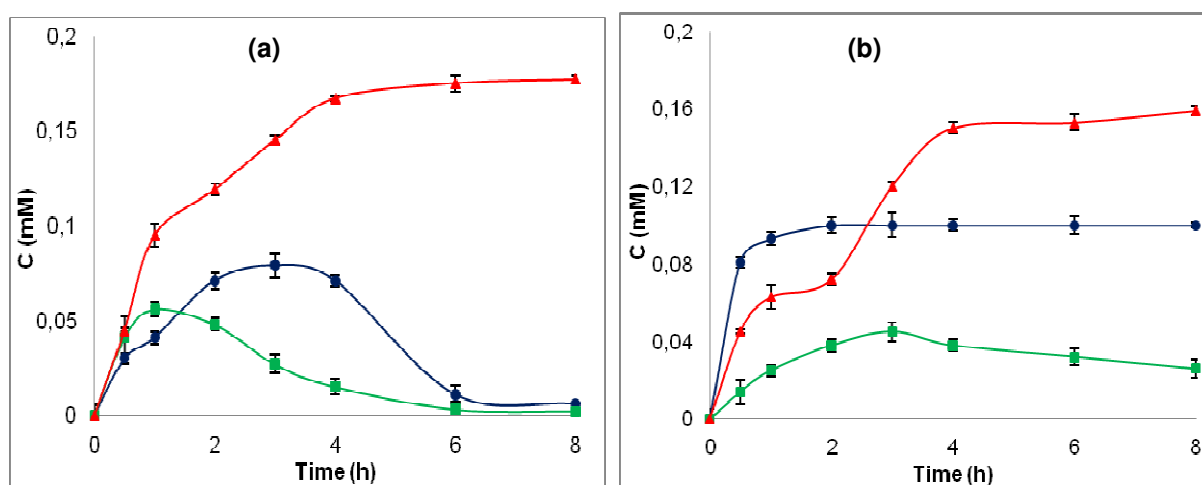


**Fig. 6-** Evolution of the inorganic ions:  $\text{Cl}^-$  (●),  $\text{NH}_4^+$  (▲) and  $\text{NO}_3^-$  (■) formed during the electro-Fenton treatment of 0.1 mM MLN solution with BDD (a) and Pt (b) anodes.  $I = 500 \text{ mA}$ .  $[\text{Fe}^{2+}] = 0.1 \text{ mM}$ ;  $[\text{K}_2\text{SO}_4] = 25 \text{ mM}$ ;  $\text{pH} = 3$ ;  $V = 230 \text{ mL}$ .

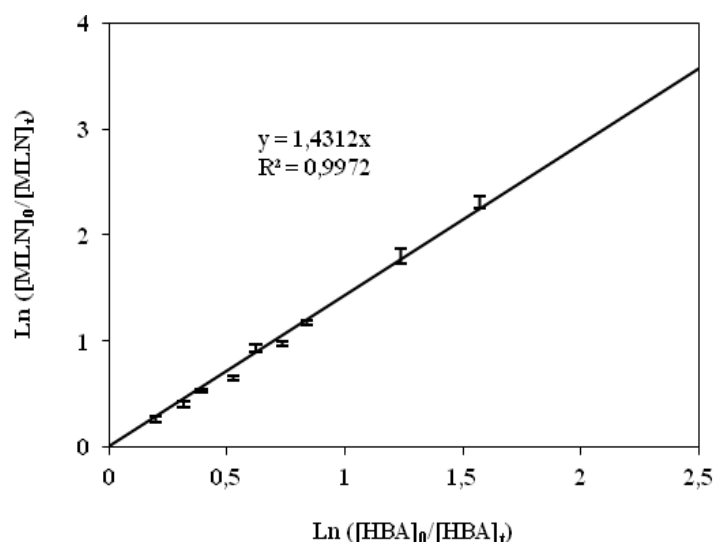


**Fig. 7-** Determination of the absolute rate constant of the MLN oxidation reaction by the hydroxyl radicals generated by the electro-Fenton process with Pt anode.  $I = 50 \text{ mA}$ ;  $[\text{Fe}^{2+}] = 0.1 \text{ mM}$ ;  $[\text{Na}_2\text{SO}_4] = 50 \text{ mM}$ ;  $\text{pH} = 3$ ;  $V = 230 \text{ mL}$ .

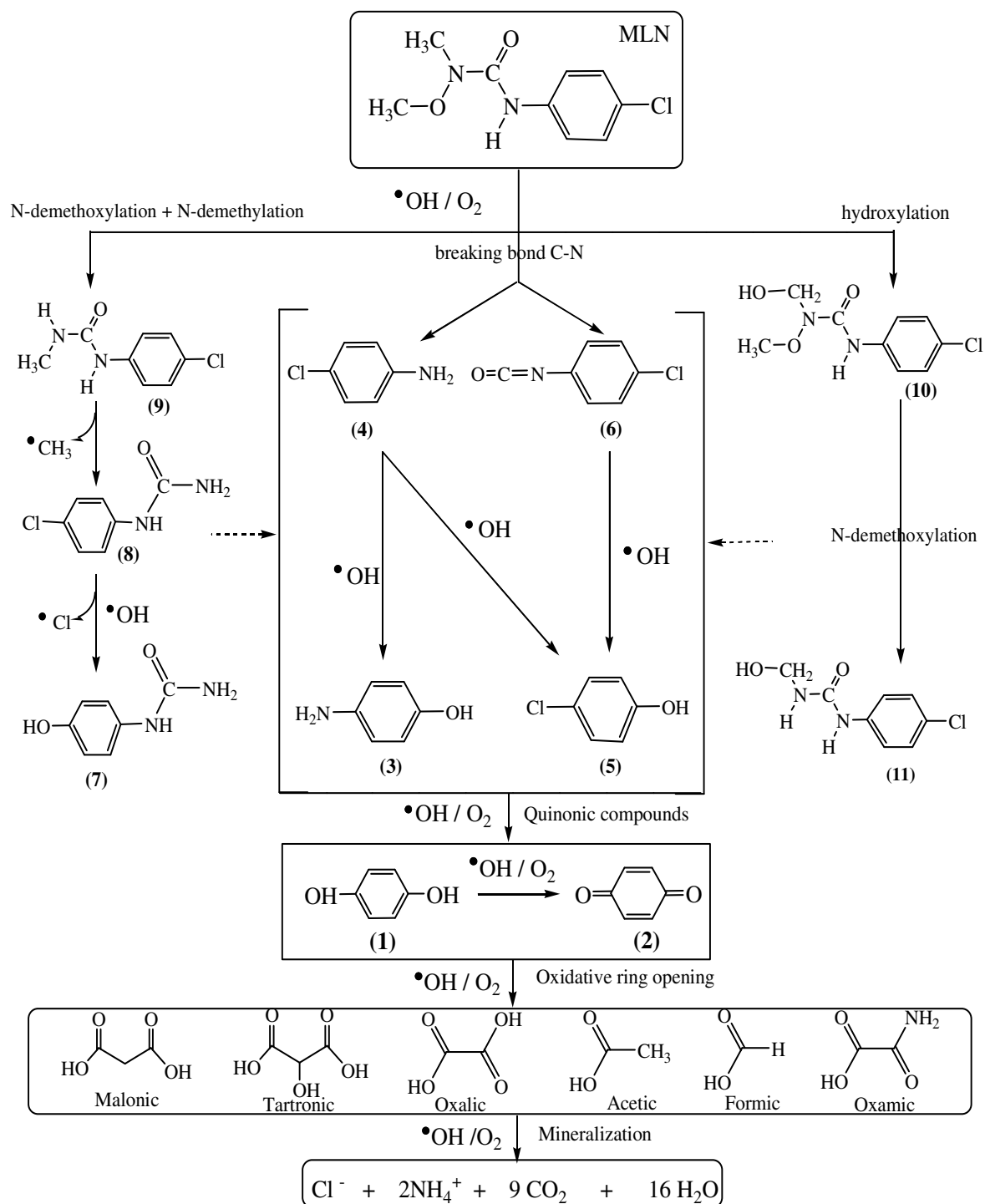


**Fig. 8-** Proposed mechanism for the mineralization of MLN in aqueous solution by the electro-Fenton process.  $[\text{FLM}]_0 = 0.1 \text{ mM}$ ,  $[\text{Fe}^{2+}] = 0.1 \text{ mM}$ ,  $\text{Na}_2\text{SO}_4$  50 mM; pH = 3, V = 230 mL, BDD anode, I = 500 mA.